

Advanced Simulation of Droplet Microfluidics

ANDREAS GRIMMER, Johannes Kepler University Linz, Austria
MEDINA HAMIDOVIĆ, Johannes Kepler University Linz, Austria
WERNER HASELMAYR, Johannes Kepler University Linz, Austria
ROBERT WILLE, Johannes Kepler University Linz, Austria

The complexity of droplet microfluidics grows with the implementation of parallel processes and multiple functionalities on a single device. This poses a severe challenge to the engineer designing the corresponding microfluidic networks. In today's design processes, the engineer relies on calculations, assumptions, simplifications, as well as his/her experiences and intuitions. In order to validate the obtained specification of the microfluidic network, usually a prototype is fabricated and physical experiments are conducted thus far. In case the design does not implement the desired functionality, this prototyping iteration is repeated – obviously resulting in an expensive and time-consuming design process. In order to avoid unnecessary debugging loops involving fabrication and testing, simulation methods could help to initially validate the specification of the microfluidic network before any prototype is fabricated. However, state-of-the-art simulation tools come with severe limitations, which prevent their utilization for practically-relevant applications. More precisely, they are often not dedicated to droplet microfluidics, cannot handle the required physical phenomena, are not publicly available, and can hardly be extended. In this work, we present an advanced simulation approach for droplet microfluidics which addresses these shortcomings and, eventually, allows to simulate practically-relevant applications. To this end, we propose a simulation framework at the one-dimensional analysis model, which directly works on the specification of the design, supports essential physical phenomena, is publicly available, and easy to extend. Evaluations and case studies demonstrate the benefits of the proposed simulator: While current state-of-the-art tools were not applicable for practically-relevant microfluidic networks, the proposed simulator allows to reduce the design time and costs e.g. of a drug screening device from one person month and USD 1200, respectively, to just a fraction of that.

CCS Concepts: • **Hardware** → **Emerging technologies**;

Additional Key Words and Phrases: Simulation, Droplet Microfluidics, 1D Analysis Model

ACM Reference Format:

Andreas Grimmer, Medina Hamidović, Werner Haselmayr, and Robert Wille. 2018. Advanced Simulation of Droplet Microfluidics. *ACM J. Emerg. Technol. Comput. Syst.*, (July 2018), 16 pages. <https://doi.org/10.1145/nnnnnnn.nnnnnnn>

1 INTRODUCTION

Droplet microfluidics is a highly dynamic and fast evolving field, whose applications target the fields of chemistry, biology, and material science [26]. These high dynamics in droplet microfluidics are demonstrated by the rapidly growing number of publications as discussed e.g. in [8]. For droplet microfluidics, two different platforms exist: in the platform which is also known as *segmented flow*

Authors' addresses: Andreas Grimmer, Johannes Kepler University Linz, Austria, andreas.grimmer@jku.at; Medina Hamidović, Johannes Kepler University Linz, Austria; Werner Haselmayr, Johannes Kepler University Linz, Austria; Robert Wille, Johannes Kepler University Linz, Austria.

Permission to make digital or hard copies of all or part of this work for personal or classroom use is granted without fee provided that copies are not made or distributed for profit or commercial advantage and that copies bear this notice and the full citation on the first page. Copyrights for components of this work owned by others than ACM must be honored. Abstracting with credit is permitted. To copy otherwise, or republish, to post on servers or to redistribute to lists, requires prior specific permission and/or a fee. Request permissions from permissions@acm.org.

© 2009 Association for Computing Machinery.

1550-4832/2018/7-ART \$15.00

<https://doi.org/10.1145/nnnnnnn.nnnnnnn>

or *two-phase flow microfluidics* [5, 35], droplets flow through closed microfluidic channels [36], while in the *digital microfluidics* platform the droplets are moved on a hydrophobic surface using electrowetting-on-dielectric [27]. In this work, we focus on the first platform.

Here, a pump produces a force which causes a flow of a continuous fluid through the microfluidic network. Into this continuous fluid, another immiscible fluid is injected (using e.g. T-junctions, Y-junctions, capillary-based devices, or flow focusing devices [5, 24]) which forms droplets. Then, the continuous flow transports the droplets through the microfluidic system consisting of channels and modules. When the microfluidic system consists of multiple paths through which the droplet can flow, the resulting designs are called *microfluidic networks*.

The design and realization of microfluidic networks is a complex task which involves the consideration of various aspects such as the geometry of the channels, the used phases, the applied pressure, and the effects of droplets. Engineers consider these aspects by conducting calculations, by trusting their experience, or even rely on their intuition. Moreover, in order to tackle the complexity, they frequently apply simplifications and assumptions, e.g. to ignore the hard to grasp effects of droplets and their corresponding collective hydrodynamic feedback. In order to support the engineer in this task, recently also first automatic methods have been presented, e.g. for dimensioning microfluidic networks [22], determining architectures [21], or the generation of droplet sequences for passive routing [23] (in the later cases, utilizing simplifications in terms of a discrete model [20]).

Once a complete specification has been derived, first a design is drawn using a CAD program (here also an automatic (online) tool [19] can support the engineer in automatically generating meander channel designs) and a prototype is fabricated next, which is used to evaluate whether the resulting design indeed implements the desired functionality or not. If this is not the case (which is likely in the first iterations), the engineer has to refine the design and continue the entire process again – including another fabrication and evaluation. This prototyping cycle is repeated until the engineer obtains a design which realizes the desired behavior. As reported e.g. in works such [7, 11], this can be a difficult, time-consuming, and expensive process.

In order to address this problem, simulation approaches utilizing the *one-dimensional (1D) analysis model* have been proposed (see e.g. [1, 3, 9, 14, 16, 25, 28–31, 33]), which aim to allow for an evaluation of the specification of the design prior to fabrication¹. The applied 1D analysis model is physically validated and is commonly used for designing and modeling droplet microfluidic networks. This model abstracts channels characterized by their height, width, and length to a single fluidic resistance value. Similarly, this model also abstracts droplets to single resistance values. While these abstractions prevent to simulate effects like droplet merging or splitting on the 1D analysis model, they allow to efficiently predict (a) the droplets' paths/trajectories through the network (this can decide which assay is executed on the droplet), (b) the flow changes caused by all droplets and the resulting impacts (e.g. distance changes between droplets, droplet patterns, etc.), and (c) the time a droplet takes to pass through the network. Using these functionalities, the design could initially be validated before the first prototype is fabricated, alternative designs could be explored (i.e. to test different dimensions of channels, applied pressures, etc.), and the design could be optimized.

However, none of the existing solutions got established in practice yet. This is caused by the fact that, despite their promises, currently available simulation solutions

¹Note that, also simulation approaches utilizing Computational Fluid Dynamics (CFD) are available. They, however, consider a high level of details and, hence, are usually not capable to simulate entire microfluidic networks. This is discussed later in Section 5.

- (1) are not dedicated to microfluidics and, therefore, first require to manually map the design to an electrical circuit or can only determine a single, static state of the microfluidic network, but do not allow to simulate the time-dynamic behavior caused by the flow of droplets as it is the case for Spice [28],
- (2) target only networks which consist of channels which branch and merge [3, 16, 29] or are even limited to networks consisting of a symmetric/asymmetric loop [1, 9, 14, 25, 30, 31, 33], but ignore essential physical phenomena such as trapping droplets, checking whether droplets are squeezed through any gaps, and clogging of channels,
- (3) are not publicly available (in fact, no tool is publicly available), and
- (4) are static, i.e. do not allow for further extensions which are essential in order to support the broad range of application scenarios engineers in the microfluidic domain are faced.

As a consequence, the design of microfluidic devices still follows the costly and time-consuming “trial-and-error” approach reviewed above.

In this work, we are introducing an advanced simulation approach which addresses these shortcomings. To this end, we propose a simulation framework which (1) directly works on the specification of the design and considers the interdependencies caused by all droplets, (2) extends the current state of the art with important physical phenomena which are required for practical designs, (3) is publicly available at http://iic.jku.at/eda/research/microfluidics_simulation/, and, (4) due to the availability of the source code and the event-based algorithm, can easily be extended to support further applications.

In the following, the proposed simulation approach is introduced and demonstrated as follows: Section 2 provides an overview of the simulation framework and describes the respectively applied 1D analysis model it is based. In Section 3, we consider physical phenomena which cannot be simulated by the previously proposed approaches covered above and discuss how support for them can easily be added to the proposed framework. In Section 4, we evaluate how the simulation framework advances the state of the art (where no simulations at all are applied) and demonstrate by means of a case study the application of the proposed framework for the design of a practically-relevant microfluidic network. More precisely, we show that using the proposed framework allows to reduce the design time and costs e.g. of the drug screening device proposed in [7] from one person month and USD 1200, respectively, to just a fraction of that. Finally, we compare the proposed simulation framework to related work and especially to simulations on other abstraction levels (e.g. CFD-simulations) in Section 5 and conclude the paper in Section 6.

2 SIMULATION FRAMEWORK

This section introduces the main working principle of the proposed simulation framework for droplet microfluidics, which is based on the *one-dimensional (1D) analysis model* as described in [28, 29] and is similar to all existing simulation approaches using this model. The 1D analysis model reduces the microfluidic network (i.e. an object in the 3D-space) to the 1D-space. In the following, we describe the general idea of the approach, i.e. how this abstraction is utilized for a fast (i.e. computationally inexpensive) simulation of droplet microfluidic networks. Based on that, the remainder of this work covers how, based on that, further physical phenomena can be added to make the simulation framework applicable for more practically-relevant microfluidic networks.

The framework describes the microfluidic network as a directed graph consisting of *nodes* and *edges*. The edges represent channels, modules, and pumps. Their direction represents the counting direction of the flow. The nodes connect the edges to each other.

The *flow state* of all the channels and the modules within such a network is then described by the Hagen-Poiseuille equation [4], i.e. by $\Delta P = RQ$, where ΔP is the *pressure difference* (in [mbar])

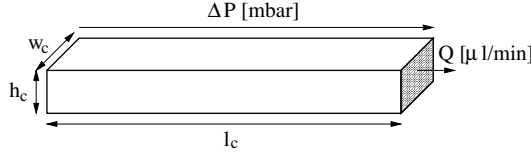


Fig. 1. Microfluidic channel

between the two end nodes of the channel/module, Q is the *volumetric flow rate* (in [$\mu\text{l}/\text{min}$]) through the channel/module, and R is the *fluidic resistance* (in [$\text{mbar}/(\mu\text{l}/\text{min})$]) posed by the channel/module. A low Reynolds number allows to reduce the resistance of channels/modules (which is defined by their geometry and the viscosity of the continuous phase μ_{cont}) to a constant value (i.e. a reduction from the 3D-space into the 1D-space). For example, the resistance R_c of a rectangular channel c (with length l_c , width w_c , and height h_c), where the ratio h_c/w_c is less than 1, is defined by [12]

$$R_c = \frac{a \mu_{cont} l_c}{w_c h_c^3}, \quad (1)$$

where a denotes a dimensionless parameter defined as

$$a = 12 \left[1 - \frac{192 h_c}{\pi^5 w_c} \tanh \left(\frac{\pi w_c}{2 h_c} \right) \right]^{-1}. \quad (2)$$

EXAMPLE 1. Consider the microfluidic channel shown in Fig. 1 with a length $l_c = 500\mu\text{m}$, a width $w_c = 120\mu\text{m}$, and a height $h_c = 60\mu\text{m}$. Furthermore, assume that the viscosity of the continuous phase is equal to $\mu_{cont} = 4.57\text{mPa}\cdot\text{s}$. This allows to determine the dimensionless parameter which is equal to $a = 17.46$ and the fluidic resistance of this channel which is equal to $R = 0.256\text{mbar}/(\mu\text{l}/\text{min})$.

Also, the pumps producing the flow through the microfluidic networks can be described in the 1D-space: A syringe pump produces a constant volumetric flow rate Q_{in} and a peristaltic pump produces a pressure gradient ΔP_{in} .

The presence of droplets in channels/modules change the flow state as they cause additional resistances. Current state-of-the-art simulation tools track the droplets as infinitely small points in the channel/module (later in Section 3.2 a more comprehensive model for droplets is introduced and applied) and a sufficiently large distance between droplets (typically a few channel sections/diameters) prevent that their flow perturbations interact [29]. These assumptions allow to model each droplet by an additional resistance, which is again a value in the 1D-space. When n droplets flow through a channel/module, the overall resistance can be calculated by

$$R^* = R_c + n R_d. \quad (3)$$

Note that the number n of droplets contained in a channel represents a specific droplet state and changes throughout the simulation.

The droplet resistance R_d has been experimentally studied in several works as e.g. [2, 12, 15]. For example, [15] established the rule that each droplet increases the resistance of the segment of the channel it occupies by 2-5 times. When using a factor of 3, the droplet resistance is described by

$$R_d = \frac{3 a \mu_{cont} L_d}{w_c h_c^3}, \quad (4)$$

where L_d is the droplet length.

Note that the abstractions in the 1D analysis model prevent to simulate details of the droplet formation in e.g. a T-junction. However, Biral et al. [3] reviewed a microfluidic setting and model for T-junctions, which allows to determine the length of the droplets and their distance. This droplet length can then be used to determine the droplet resistances.

In order to determine the flow states in all edges, the framework automatically applies the mass conservation at each node of the graph and the relation described by the Hagen-Poiseuille equation [29]. The obtained equations are similar to the well-known Kirchhoff's law and can be directly transferred when we map the Hagen-Poiseuille equation to the *Ohm's law* with $V = RI$ (where the voltage V corresponds to the pressure gradient ΔP , the current I corresponds to the volumetric flow rate Q , and the resistance R of a conductor corresponds to the fluidic resistance R). More precisely,

- the sum of flow rates into a node is equal to the sum of flow rates out of that node and
- the directed sum of pressure gradients around any closed cycle in the graph is zero.

By solving the obtained equation system, the framework derives the flow state (i.e. ΔP and Q) in every channel and module for the *current* droplet positions. The obtained flow rates in the channels/modules determine the *current* speed of the droplet by $v_d = \alpha \cdot Q / (w_c h_c)$, where α is the slip factor. Under the conditions where the droplet length is between 1.5 and $7.2 \cdot w_c$, the viscosity ratios 0.03 or 0.88, and the capillary number between 0.001 and 0.01 without surfactant, Vanapalli et al. [37] found the slip factor to be constant and equal to $\alpha = 1.28$.

Using this model, the framework can predict the traffic of droplets, i.e. when a droplet arrives at a bifurcation, it chooses the branch with the instantaneous highest flow rate [10, 14, 25] and does not split (this is true at a low capillary number because the surface tension dominates the viscous stress).

The introduced equations allow to determine the flow state as well as droplet velocities for a specific droplet state and, hence, update the system state including the droplet positions. The respectively obtained flow state is valid until

- a new droplet is injected (adds a resistance),
- any droplet leaves the network (removes a resistance), or
- any droplet enters another edge (causes a shift of the resistance).

Hence, as soon as any of those *events* occurs, the current flow state becomes invalid and the simulation framework re-calculates the flow state (i.e. newly added, removed, or changed resistances are incorporated into the equation system which, afterwards, is re-solved). These event-based calculations make the framework suitable to efficiently simulate large microfluidic networks.

Overall, this provides the basic principle of an efficient simulation of droplet-based microfluidic networks (abstracting the channels and droplets to 1D values, use the Hagen-Poiseuille and mass conservation laws to determine the flow state in all channels/modules, update the droplet positions, and adjust/re-evaluate the equation system for the next event). However, this state of the art simulation approach only provides the basis for simulating droplets flowing through networks consisting of channels which branch and merge (exploiting the fact that a droplet always flows into the branch with the highest instantaneous flow rate). But it does not yet support the simulation of droplets on which actual operations are executed. How this framework can be extended with the correspondingly required physical phenomena is covered in the next section.

3 ADVANCED SIMULATION FRAMEWORK

This section describes how more advanced physical phenomena can be simulated using the proposed framework. We are illustrating that by representative (and practically-relevant) examples from the literature, i.e. proposed designs introduced in the recent past which have been designed without

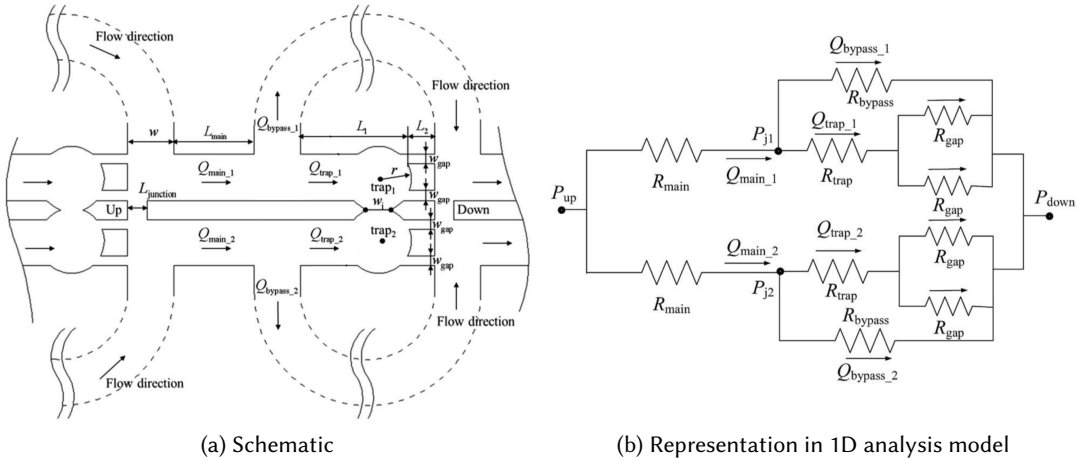


Fig. 2. Trapping well proposed in [7]²

simulation support (as current simulators were not suited). To this end, we first review those designs and what phenomena were missing in existing simulation approaches to properly simulate them. Afterwards, we describe how support for those phenomena is integrated into the framework eventually allowing for simulating these designs.

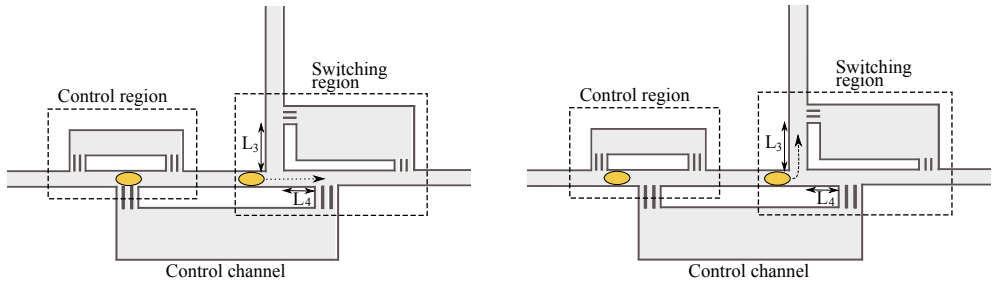
3.1 Unsupported Phenomena

An important operation in experiments is to *trap* droplets as these trapped droplets allow to precisely control the reaction time or to observe particle-particle interactions [7, 39]. Fig. 2a shows a schematic of two connected trapping wells, which entirely work passively (i.e. only hydrodynamic effects and no external components for control are used) and has been proposed in [7]. If one of the trapping wells (denoted “trap₁” and “trap₂” in Fig. 2a) does not yet contain a droplet, the first arriving droplet is trapped. As soon as it contains a droplet, all following droplets do not enter the trapping well anymore and are bypassed (i.e. flow through the channel which is indicated by dashed lines in Fig. 2a). Therefore, the design ensures that the trapped droplet clogs the two narrow channels (i.e. the gaps in Fig. 2a with width w_{gap}) so that the flow into the bypass channel is higher. Additionally, for a correct analysis of two trapped and merged droplets, the design has to ensure that these droplets are not squeezed through the two narrow channels.

Furthermore, Fig. 2b shows how this trapping well is mapped to a directed graph. More precisely, this figure shows that the 1D analysis model abstracts each channel by its fluidic resistance R (i.e. the edges of the graph). Moreover, the directions of the edges represent the counting directions of the volumetric flows. The nodes in the graph connect these edges.

Besides trapping wells, switches are essential in many applications in order to control the path of droplets. In [6], the switch shown in Fig. 3 has been recently proposed, which is capable to route multi-droplet frames. This switch uses the effect that the presence of a droplet at the input of a narrow channel causes a blocking of the flow into this channel (i.e. the droplet *clogs* the channel). Fig. 3a shows a state where the droplet in the “Control region” clogs the flow into the channel downwards. This cut of the flow controls the second droplet in the “Switching region”, i.e. this cut of the flow routes this droplet into the channel to the east, which is depicted by the arrow in Fig. 3a.

²Published by The Royal Society of Chemistry.



(a) The droplet in the “Control region” clogs the flow into the “Control channel”, which routes the droplet in the “Switching region” into the channel to the east.

(b) The droplet in the “Control region” does not clog the flow into the “Control channel”, which routes the droplet in the “Switching region” into the channel to the north.

Fig. 3. Multi-droplet switch proposed in [6]

In contrast, Fig. 3b shows another state where the droplet in the “Control region” does not clog the flow into the channel downwards. This causes the second droplet in the “Switching region” to enter the channel to the north, which again is depicted by the arrow in Fig. 3b. All details, how this switch exploits the clogging of the flow in order to route droplets are described in [6].

However, in order to simulate these operations, the simulation of further physical phenomena is required, namely whether droplets

- are *trapped* in the microfluidic network,
- are *squeezed* through any gap, or
- are *clogging* a channel.

Using the “basic” framework introduced in the previous section, none of these phenomena and, hence, none of the operations can properly be simulated. Since also all related work proposed thus far does not provide support for that, the practically-relevant applications discussed in [6, 7] cannot be simulated thus far.

3.2 Implementation of the Phenomena

In order to support these physical phenomena and, by this, allow for the simulation of practically-relevant applications such as those discussed above, we extend the introduced framework with new equations and events. These new events demonstrate how the presented framework allows for easy extensions – here in the form of the following three events:

Droplet Trapped Event: A droplet is trapped in the microfluidic network when it stops in an edge. As long as a trapped droplet is not pushed further (e.g. by a change of the pressure), it stays in the edge (potentially until the end of the simulation). In the framework, this event is triggered when a droplet is contained in an edge (i.e. a channel or module), which does not have a successor edge through which the droplet can leave this edge (cf. the next event implements the check whether a droplet is pushed out of an edge).

EXAMPLE 2. Fig. 4 shows a schematic of a trapping well with two narrow successor channels (i.e. having small widths), which prevent the trapped droplet to enter. When a droplet is entirely contained in the trapping well, the respective event is triggered.

Droplet Squeezed Through Gap Event: The *Young-Laplace pressure* gives the pressure difference between the inside and the outside of a droplet. This often merely called Laplace pressure is

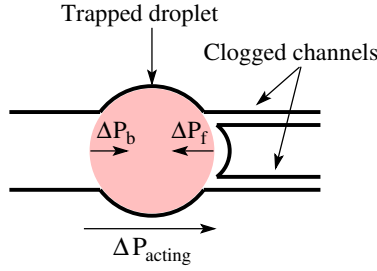


Fig. 4. Schematic of a trapped droplet

given for a not squared droplet by [32]

$$\Delta P_{Lap} = \gamma \left(\frac{1}{r_y} + \frac{1}{r_z} \right), \quad (5)$$

where γ is the interfacial tension (in $[mN/m]$) and r_y and r_z are the radii of the curvature of the droplet.

The difference in the Laplace pressure generated at the front (denoted by f) and back (denoted by b) of the droplet is given by

$$\Delta P_{Lap} = \gamma \left[\left(\frac{1}{r_{y,f}} + \frac{1}{r_{z,f}} \right) - \left(\frac{1}{r_{y,b}} + \frac{1}{r_{z,b}} \right) \right]. \quad (6)$$

Fig. 4 shows the corresponding Laplace pressures at the front and back of the droplet.

The Laplace pressure can now be used to predict, whether a droplet is squeezed through a gap. More precisely, a droplet is squeezed through a gap when the applied pressure exceeds the Laplace pressure.

EXAMPLE 3. Consider again the trap shown in Fig. 4. Here, the difference in the Laplace pressure generated at the front and back can be derived from Eq. 6 and is given by [7]

$$\Delta P_{Lap} = \gamma \left[\left(\frac{2}{w_{gap}} + \frac{2}{h_c} \right) - \left(\frac{1}{r_d} + \frac{2}{h_c} \right) \right], \quad (7)$$

where w_{gap} is the width of the gap shown in Figure 2a, and r_d is the droplet radius in the trap.

When the pressure ΔP_{acting} acting on the droplet is smaller than the Laplace pressure, the droplet stays in the trap, i.e.

$$\Delta P_{acting} < \Delta P_{Lap} \quad (8)$$

has to be fulfilled that the droplet is not squeezed through any gap (and, therefore, stays in the trap).

As the pressure acting on the droplet changes in each system state, checking whether a droplet is squeezed through any gap has to be done for all system states. Therefore, the simulation framework is extended so that every time a new system state is determined, the obtained pressures are checked whether they exceed the Young-Laplace pressures. If so, a corresponding event is triggered and the simulation framework reports this to the engineer and terminates the simulation.

Droplet Starts/Ends Clogging Event:

A droplet clogs the flow into an edge when it blocks the input of this edge but does not enter this edge. In both of the microfluidic networks discussed in Section 3.1, droplets are used to clog the flow: In the network proposed in [7], a trapped droplet is pushed by the pressure against two narrow gaps and, hence, clogs the flow into these narrow gaps (cf. the trapping well in Fig. 4). In

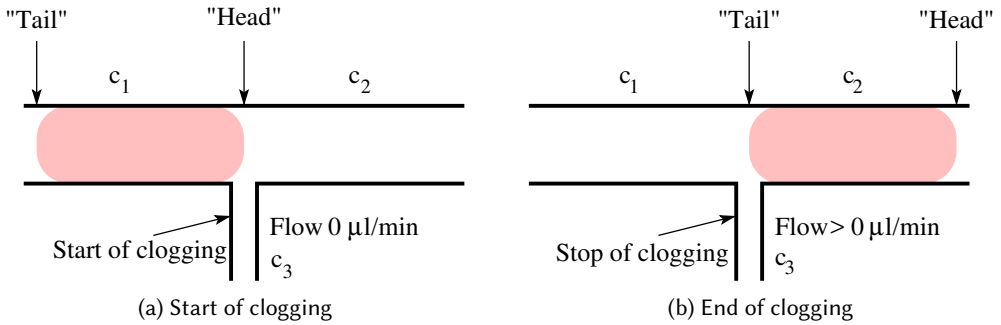


Fig. 5. Clogging time span

the switch proposed in [6], the flow into the perpendicular channel (cf. the channel arrangement in Fig. 5) is clogged when a droplet passes.

However, the geometric information which is required to decide whether a droplet can clog a channel is not available in the applied model as it abstracts the 3D-network to 1D-values. Therefore, we extend the simulator with a new edge type, i.e. with *cloggable edges*. These cloggable edges allow to model that a passing or trapped droplet blocks the flow into this edge. More precisely, the flow into a cloggable edge is blocked in the following two cases: First, when a cloggable edge and an edge containing a trapped droplet are connected to the same node (i.e. the trapped droplet clogs the flow, cf. the trapping well). Second, when a cloggable edge is connected to a node through which a droplet passes (i.e. the droplet temporary clogs the flow, cf. the switch). When the user describes the microfluidic network and especially its channels in the simulation framework, he/she can choose between normal and cloggable channels.

In order to implement this clogging in the simulation framework, information about the time span when the droplet clogs the channel is required. However, this information is not yet available in the framework as presented in Section 2 because the underlying model tracks the droplets as infinitely small points. This is a disadvantage of this model and, therefore, also of state-of-the-art simulation tools, which limits the practicality of the state of the art.

In order to allow clogging in the proposed simulation framework, we extend the model with position information of droplets, i.e. the framework tracks the position of the “head” and the “tail” of the droplet. More precisely, this additional position information allows to extend the framework with two new events which are triggered when a droplet starts or stops clogging a channel.

EXAMPLE 4. Fig. 5 shows two states of a droplet flowing along a channel. During these two states, the narrow channel is clogged by the droplet and, therefore, the flow into this channel is blocked. Here, the framework first triggers an event when the “head” of the droplet is located over the narrow channel, which starts the clogging. Later, when the “tail” of the droplet is over the narrow channel, the framework triggers another event which stops the clogging. For these two events, the enriched model containing the position information of droplets is used.

These two events give the time span when a droplet clogs a channel. In order to implement the blocking of the flow into the clogged edge, the underlying graph representing the microfluidic network needs to be dynamically changed. More precisely, when an event is triggered to start the clogging, the respective edge is removed from the graph. Similarly, when an event is triggered to stop the clogging, the respective edge is again added to the graph. These dynamic changes require a

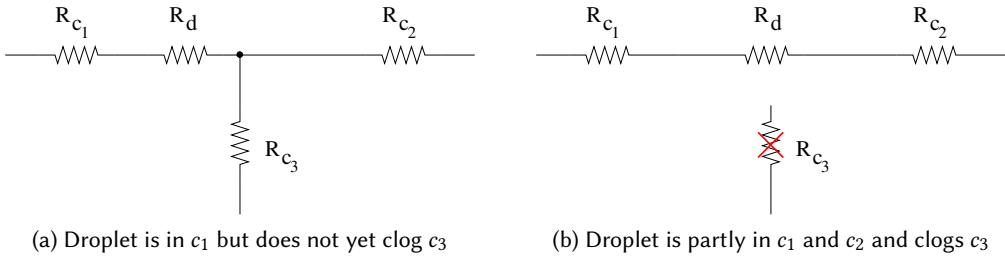


Fig. 6. Changes during clogging in the graph describing the microfluidic network

re-analysis of the underlying graph, the derivation of a new equation system, and the re-calculation of the flow states.

EXAMPLE 5. Consider again the network shown in Fig. 5. Fig. 6 shows how this network is represented as a graph. More precisely, Fig. 6a shows a state where a droplet with resistance R_d flows in channel c_1 . In this state, the droplet is not yet located over the narrow channel c_3 and, hence, the flow can enter c_3 . Fig. 6b shows a state where the droplet is above channel c_3 and, hence, clogs the flow into this channel. Therefore, when the event is triggered to start the clogging, the edge representing channel c_3 is removed from the underlying graph. This removal of an edge entirely cuts the flow into channel c_3 . Similarly, when the event is triggered to stop the clogging, the edge representing channel c_3 is again added to the underlying graph.

3.3 Overall Algorithm

The proposed simulation framework takes a description of a microfluidic network as input and automatically derives, applies, and solves the resulting equation systems. For solving the equation system, a lower-upper (LU) decomposition [17] is used, which results in a polynomial time complexity with respect to the size of the equation system. The size of the equation system depends on the size of the microfluidic network.

This equation system has to be re-solved when any of the events discussed above is triggered by any droplet. More precisely, an event is triggered when

- a new droplet is injected,
- a droplet leaves the network,
- a droplet enters another edge,
- a droplet is trapped in the microfluidic network,
- a droplet is squeezed through any gap (which usually terminates the simulation), and
- a droplet starts or stops clogging a channel.

Overall, these event-based re-calculations of the equation system make the proposed advanced simulation framework very efficient. This allows to simulate large microfluidic networks within negligible computation times.

4 EVALUATION AND CASE STUDY

The simulation framework proposed above as well as a corresponding graphical user interface has been implemented in Java (which makes the framework platform-independent) and made publicly available at http://iic.jku.at/eda/research/microfluidics_simulation/. The resulting tool addresses the main shortcomings of the current state of the art (reviewed in Section 1) e.g. by being

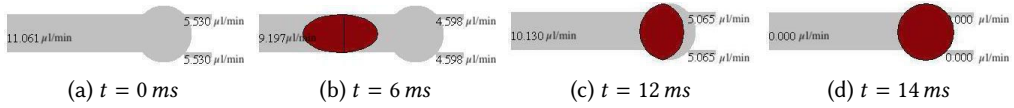


Fig. 7. The framework simulates a trapped droplet, checks the Young-Laplace pressure, and clogs the flow into the gaps.

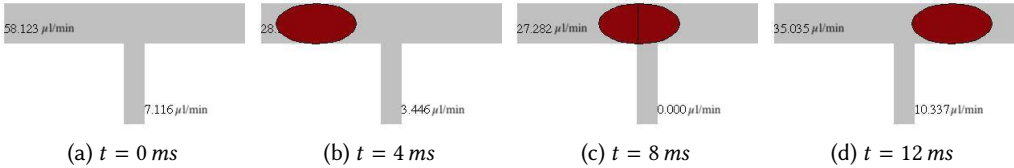


Fig. 8. The framework simulates the clogging using the “head” and “tail” position information of the droplet.

- dedicated to droplet microfluidics (it allows to simulate the time-dynamic behavior caused by the flow of droplets as well as it directly uses the specification of the microfluidic network, which is both unsupported by Spice),
- applicable for practically-relevant networks as the framework now supports important physical phenomena,
- publicly available, and
- easily accessible and extendible.

By this, the resulting framework has the potential to establish simulation in the design of droplet microfluidics – eventually allowing to avoid unnecessary “trial-and-error” iterations with costly and time-consuming physical fabrications.

In order to confirm that, intensive evaluations have been conducted, which consist of tests for the unsupported phenomena and the application of the framework for a case study using the microfluidic network of [7]. In the following, we summarize the most important evaluations.

4.1 Evaluation of the Phenomena

A main characteristic of the proposed simulation framework (which is essential to make the approach broadly applicable for practically-relevant applications as discussed in Section 3.1) is its direct support of several physical phenomena which have not been supported yet. To demonstrate the working principle of the proposed simulator, we set up small networks to be simulated which require the corresponding features. More precisely, we consider (1) a network composed of a channel connected to a single trapping well and (2) a network composed of a channel to which a perpendicular channel is connected. For both networks, we used similar specifications, which are summarized in Table 1.

The accordingly obtained simulation results are respectively provided in Fig. 7 and Fig. 8 for selected time steps. The figures show the determined position of a droplet at each particular time as well as the instantaneous flow rates (provided in $\mu\text{l}/\text{min}$) in each channel.

We can observe in Fig. 7 that the droplet is successfully trapped in the trapping well. Then, the droplet stays in the trapping well, since the Young-Laplace pressure is equal to 50.4mBar (i.e. as the droplet entirely fills the trapping well, the trapping well radius is equal to the droplet radius), which is larger than the applied pressure of 30mBar . Hence, the droplet is not squeezed out through

Channel height	53 μ m
Channel width	100 μ m
Trapping well radius	75 μ m
Gap width	15 μ m
Perpendicular channel width	30 μ m
Applied pressure	30mBar
Continuous phase (silicone oil)	4.565mPa s
Dispersed phase (water)	1mP s
Interfacial tension	42mN/m

Table 1. Specification

ID	L_{bypass}	w_{gap}	Simulation results
1	3000 μ m	15 μ m	No reliable trapping
2	4000 μ m	15 μ m	-
3	5000 μ m	15 μ m	Bypass length decreases throughput
4	3000 μ m	25 μ m	Sensitive to high input pressures
5	4000 μ m	25 μ m	Sensitive to high input pressures
6	5000 μ m	25 μ m	Sensitive to high input pressures, bypass length decreases throughput

Table 2. Reliability

any of the two gaps. Furthermore, as soon as the droplet is entirely contained in the trapping well (i.e. after 14 ms), it blocks the flow into the two narrow channels.

Fig. 8 shows that a droplet over a perpendicular channel blocks the flow into this channel. The simulation framework uses the position of the droplet’s “head” and “tail” in order to determine the time span when the droplet clogs the channel.

Overall, these two small networks confirm the correct implementation of the phenomena, which is heavily utilized in the following case study.

4.2 Case Study

In this case study, we demonstrate the applicability of the proposed simulation framework to a practically-relevant application. More precisely, we consider the design of the microfluidic network proposed in [7]. This microfluidic network is developed to screen drug compounds that inhibit the tau-peptide aggregation, which is a phenomenon related to neurodegenerative disorders such as Alzheimer’s disease [34]. For the drug screening, the droplets of different content have to be trapped and merged on demand, which eventually allows a precise control of the reaction time. The working principle is purely passive (i.e. no valves or other active components are used) and it is illustrated by means of videos available at <https://doi.org/10.1039/C7RA02336G>. In the following, we first review the design process of this microfluidic network which has been conducted without any simulations (according to [7]). Afterwards, we show how the proposed simulation framework can help here.

For deriving the specification (i.e. the channel dimensions, applied pressures, etc.), the engineer conducted calculations and applied simplifications as well as assumptions. For example, the engineer simplified the effects of droplets because it is impossible to consider those by hand. As the effects of all simplifications and assumptions cannot be assessed, the engineer came up with six different specifications, which have three different bypass channel lengths (i.e. droplets pass this channel when the respective trapping well already contains a droplet) and two different gap sizes. Table 2 shows the resulting specifications. In order to validate the functionality of these specifications, the engineer fabricated prototypes and conducted physical experiments. In fact, the engineer had no other choice as no simulation tools were available which would have been capable to handle the required phenomena (CFD simulations are too computationally expensive for complete microfluidic networks, cf. Section 5, and other state-of-the-art simulations are not applicable). Finally, the engineer picked the specification trapping the droplets in the most reliable way. The engineer reported that the fabrication and testing of these six prototypes resulted in one person month of manual labor and financial costs of USD 1200.

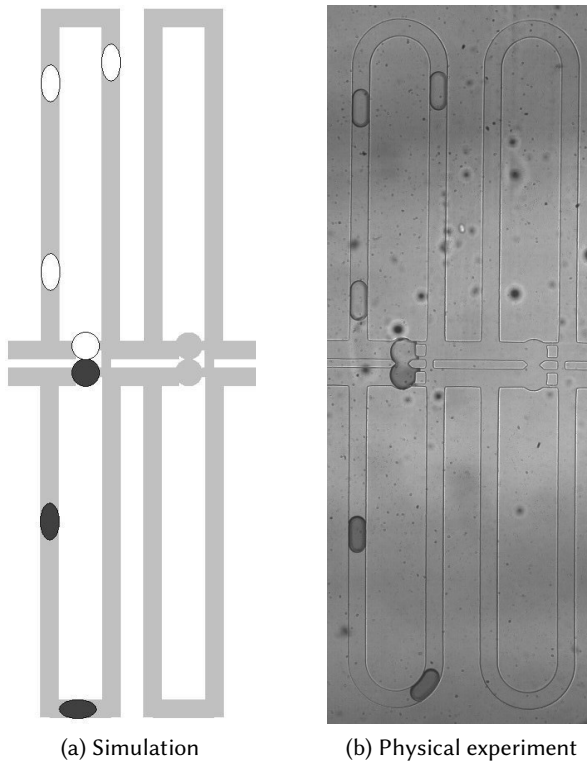


Fig. 9. Comparison of the simulation with the physical experiment

In our case study, we revisited this design process and additionally applied the proposed simulation framework. Therefore, the different designs were validated and tested using the framework *before* any physical experiments are conducted. We set up simulations of the six different specifications (cf. Table 2). Then, we analyzed the obtained simulation results with respect to the taken path of droplets, the flow rates, whether droplets are unintentionally squeezed through any gap, and how long it takes until a droplet is trapped. For all specifications, we observe the intended paths of the droplets. But for the specification with ID 1, the simulation shows that the flow rates do not allow a reliable trapping of droplets (i.e. the flow into the trapping well was hardly larger than the flow into the bypass). Next, we simulated different input pressures. Generally, too high input pressures cause the droplet to be squeezed out of the trapping wells. But we found that especially the specifications with the larger gap widths (specified with ID 4-6) are more sensitive to higher pressures (i.e. a larger gap width reduces the Young-Laplace pressure). Finally, we measured the time until a droplet is trapped as this is especially relevant for bio-assays with cells. Here, the simulations show that, the longer the bypass channel, the longer the time until a droplet is trapped. All those effects have also been observed in the physical experiments (but, therefore, six prototypes were necessary).

Table 2 summarizes the obtained results, which show a clear preference for the second specification. This specification is the one which was eventually realized in [7]. For this specification, we provide a video showing the output of the simulator under <https://youtu.be/f5v9KIGIQB4>. Additionally, we compare the simulator's output with photos of a physical experiment captured

with a frequency of 50 *fps*. Additionally, Fig. 9 shows the simulation and the physical experiment for a certain time point.

This simulation predicts the same functionality as the corresponding physical experiment, which finally allows the utilizing of the simulator to evaluate different specifications. The simulation setup of the considered microfluidic network was hardly any work compared to fabricating devices. Furthermore, all simulation runs were completed on a standard desktop PC within at most three seconds. Overall, the use of the simulation framework in the design process can reduce the number of fabricated devices to a single one, and hence, would allow to reduce the design time and costs of this drug screening device from one person month and USD 1200, respectively, to just a fraction of that. A more detailed description of this case study is available at [18].

5 COMPARISON TO RELATED WORK

In this section, we compare the proposed framework to other simulation tools and levels. Basically, simulation approaches for droplet microfluidics can be classified into two abstraction levels:

- *Simulations using Computational Fluid Dynamics (CFD)*: Tools like *Comsol Multiphysics*, *Ansys*, or *OpenFoam* employ CFD simulations. Comprehensive reviews of the methods and tools are provided in [13, 40]. These tools simulate the fluid flow in the most accurate way, i.e. allow to simulate turbulences and effects like droplet deformation and splitting. But therefore, they require a complex simulation setup (e.g. the generation of a mesh based on the physical design). Furthermore, the high level of physical details causes significant computational costs, which yield simulation results of high precision but also limits their applicability to small designs and single components. For example, these methods are inappropriate to quickly simulate practically large-scale microfluidic networks [28] and, therefore, recently a hybrid solution was presented in [38], which queries precomputed results from a database and combines it with simulations based on the 1D analysis model.
- *Simulations on the 1D analysis model*: This model is applied in the presented simulation framework and was introduced in Section 2. The model is valid when the flow is laminar, viscous, and incompressible [29]. The abstraction of the microfluidic network to 1D values makes the simulation efficient as only linear equations need to be solved, which makes corresponding simulators most suitable for practical large-scale microfluidic networks. These simulations are especially useful for determining the paths and position of droplets, the time a droplet takes to pass through the network, as well as for parametric analysis needed to validate and optimize designs. However, as discussed in Section 1, existing methods within this category (e.g. [1, 3, 9, 14, 16, 25, 29–31, 33]) suffer from limitations such as poor applicability to the microfluidic domain, missing support for essential physical phenomena, their non-availability, and their rather static and, hence, not extendible nature. In this work, these shortcomings have been addressed by the advanced simulation framework.

6 CONCLUSION

In this paper, we presented an advanced simulation framework which addresses severe limitations of state-of-the-art simulators by being dedicated to droplet microfluidics and by addressing essential physical phenomena, which are required for practically-relevant applications. Furthermore, the open-source implementation allows for a broad application of the framework and even further extensions. The resulting framework can be applied by engineers in order to validate their design before even the first prototype is made. That these simulations can save costs as well as time has been shown in a case study for a microfluidic network which is used to screening drug compounds

that inhibit the tau-peptide aggregation, a phenomenon related to neurodegenerative disorders such as Alzheimer's disease.

REFERENCES

- [1] Mehran Djalali Behzad, Hamed Seyed-Allaei, and Mohammad Reza Ejtehad. 2010. Simulation of droplet trains in microfluidic networks. *Phys. Rev. E* 82, 3 (2010), 037303.
- [2] Andrea Biral and Andrea Zanella. 2013. Introducing purely hydrodynamic networking functionalities into microfluidic systems. *Nano Commun. Netw.* 4, 4 (2013), 205–215.
- [3] Andrea Biral, Davide Zordan, and Andrea Zanella. 2015. Modeling, Simulation and Experimentation of Droplet-Based Microfluidic Networks. *Mol. Biol. Multi-scale Commun.* 1, 2 (2015), 122–134.
- [4] Henrik Bruus. 2008. *Theoretical microfluidics*. Vol. 18. Oxford university press Oxford.
- [5] Xavier Casadevall i Solvas and Andrew deMello. 2011. Droplet microfluidics: recent developments and future applications. *Chem. Commun.* 47, 7 (2011), 1936–1942.
- [6] Gaetano Castorina, Marco Reno, Laura Galluccio, and Alfio Lombardo. 2017. Microfluidic networking: Switching multidroplet frames to improve signaling overhead. *Nano Commun. Netw.* 14 (2017), 48–59.
- [7] Xiaoming Chen and Carolyn L Ren. 2017. A microfluidic chip integrated with droplet generation, pairing, trapping, merging, mixing and releasing. *RSC Adv.* 7, 27 (2017), 16738–16750.
- [8] Wei-Lung Chou, Pee-Yew Lee, Cing-Long Yang, Wen-Ying Huang, and Yung-Sheng Lin. 2015. Recent advances in applications of droplet microfluidics. *Micromachines* 6, 9 (2015), 1249–1271.
- [9] Olgierd Cybulski and Piotr Garstecki. 2010. Dynamic memory in a microfluidic system of droplets traveling through a simple network of microchannels. *Lab Chip* 10, 4 (2010), 484–493.
- [10] Wilfried Engl, Matthieu Roche, Annie Colin, Pascal Panizza, and Armand Ajdari. 2005. Droplet traffic at a simple junction at low capillary numbers. *Phys. Rev. Lett.* 95, 20 (2005), 208304.
- [11] David Erickson. 2005. Towards numerical prototyping of labs-on-chip: modeling for integrated microfluidic devices. *Microfluid. Nanofluid.* 1, 4 (2005), 301–318.
- [12] Michael J Fuerstman, Ann Lai, Meghan E Thurlow, Sergey S Shevkoplyas, Howard A Stone, and George M Whitesides. 2007. The pressure drop along rectangular microchannels containing bubbles. *Lab Chip* 7, 11 (2007), 1479–1489.
- [13] Thomas Glatzel, Christian Litterst, Claudio Cupelli, Timo Lindemann, Christian Moosmann, Remigius Niekrawietz, Wolfgang Streule, Roland Zengerle, and Peter Koltay. 2008. Computational fluid dynamics (CFD) software tools for microfluidic applications—A case study. *Comp. Fluids* 37, 3 (2008), 218–235.
- [14] Tomasz Glowdel, Caglar Elbuken, and Carolyn Ren. 2011. Passive droplet trafficking at microfluidic junctions under geometric and flow asymmetries. *Lab Chip* 11, 22 (2011), 3774–3784.
- [15] Tomasz Glowdel and Carolyn L Ren. 2012. Global network design for robust operation of microfluidic droplet generators with pressure-driven flow. *Microfluid. Nanofluid.* 13, 3 (2012), 469–480.
- [16] Nils Gleichmann, Daniéll Malsch, Peter Horbert, and Thomas Henkel. 2015. Toward microfluidic design automation: a new system simulation toolkit for the in silico evaluation of droplet-based lab-on-a-chip systems. *Microfluid. Nanofluid.* 18, 5-6 (2015), 1095–1105.
- [17] Gene H Golub and Charles F Van Loan. 2012. *Matrix computations*. Vol. 3. JHU Press.
- [18] Andreas Grimmer, Xiaoming Chen, Medina Hamidović, Werner Haselmayr, Carolyn L. Ren, and Robert Wille. 2018. Simulation before fabrication: a case study on the utilization of simulators for the design of droplet microfluidic networks. *RSC Adv.* 8 (2018), 34733–34742. Issue 60. <https://doi.org/10.1039/C8RA05531A>
- [19] Andreas Grimmer, Philipp Frank, Philipp Ebner, Sebastian Häfner, Andreas Richter, and Robert Wille. 2018. Meander Designer: Automatically Generating Meander Channel Designs. *Micromachines* 9, 12 (2018).
- [20] Andreas Grimmer, Werner Haselmayr, Andreas Springer, and Robert Wille. 2017. A Discrete Model for Networked Labs-on-Chips: Linking the Physical World to Design Automation. In *Design Automation Conference*. 50:1–50:6.
- [21] Andreas Grimmer, Werner Haselmayr, Andreas Springer, and Robert Wille. 2018. Design of Application-specific Architectures for Networked Labs-on-Chips. *Comput.-Aided Des. Integr. Circuits Syst.* 37, 1 (2018), 193–202.
- [22] Andreas Grimmer, Werner Haselmayr, and Robert Wille. 2018. Automated Dimensioning of Networked Labs-on-Chip. *Comput.-Aided Des. Integr. Circuits Syst.* (2018). <https://doi.org/10.1109/TCAD.2018.2834402>
- [23] Andreas Grimmer, Werner Haselmayr, and Robert Wille. 2019. Automatic Droplet Sequence Generation for Microfluidic Networks with Passive Droplet Routing. *Comput.-Aided Des. Integr. Circuits Syst.* (2019).
- [24] Hao Gu, Michel HG Duits, and Frieder Mugele. 2011. Droplets formation and merging in two-phase flow microfluidics. *Mol. Sci.* 12, 4 (2011), 2572–2597.
- [25] Fabien Jousse, Robert Farr, Darren R Link, Michael J Fuerstman, and Piotr Garstecki. 2006. Bifurcation of droplet flows within capillaries. *Phys. Rev. E* 74, 3 (2006), 036311.

- [26] TS Kaminski and P Garstecki. 2017. Controlled droplet microfluidic systems for multistep chemical and biological assays. *Chem. Soc. Rev.* 46, 20 (2017), 6210–6226.
- [27] Junghoon Lee, Hyejin Moon, Jesse Fowler, Thomas Schoellhammer, and Chang-Jin Kim. 2002. Electrowetting and electrowetting-on-dielectric for microscale liquid handling. *Sens. Actuators A: Phys.* 95, 2-3 (2002), 259–268.
- [28] Kwang W Oh, Kangsun Lee, Byungwook Ahn, and Edward P Furlani. 2012. Design of pressure-driven microfluidic networks using electric circuit analogy. *Lab Chip* 12, 3 (2012), 515–545.
- [29] Michael Schindler and Armand Ajdari. 2008. Droplet traffic in microfluidic networks: A simple model for understanding and designing. *Phys. Rev. Lett.* 100, 4 (2008), 044501.
- [30] DA Sessoms, Axelle Amon, Laurent Courbin, and Pascal Panizza. 2010. Complex dynamics of droplet traffic in a bifurcating microfluidic channel: Periodicity, multistability, and selection rules. *Phys. Rev. Lett.* 105, 15 (2010), 154501.
- [31] DA Sessoms, Malika Belloul, Wilfried Engl, M Roche, L Courbin, and P Panizza. 2009. Droplet motion in microfluidic networks: Hydrodynamic interactions and pressure-drop measurements. *Phys. Rev. E* 80, 1 (2009), 016317.
- [32] Melinda G Simon, Robert Lin, Jeffrey S Fisher, and Abraham P Lee. 2012. A Laplace pressure based microfluidic trap for passive droplet trapping and controlled release. *Biomicrofluidics* 6, 1 (2012), 014110.
- [33] Bradford J Smith and Donald P Gaver III. 2010. Agent-based simulations of complex droplet pattern formation in a two-branch microfluidic network. *Lab Chip* 10, 3 (2010), 303–312.
- [34] Claudio Soto. 2003. Unfolding the role of protein misfolding in neurodegenerative diseases. *Nat. Rev. Neurosci.* 4, 1 (2003), 49.
- [35] Claire E Stanley, Robert CR Wootton, and Andrew J deMello. 2012. Continuous and segmented flow microfluidics: Applications in high-throughput chemistry and biology. *CHIMIA* 66, 3 (2012), 88–98.
- [36] Shia-Yen Teh, Robert Lin, Lung-Hsin Hung, and Abraham P Lee. 2008. Droplet microfluidics. *Lab Chip* 8 (2008), 198–220. Issue 2.
- [37] Siva A Vanapalli, Arun G Banpurkar, Dirk van den Ende, Michel HG Duits, and Frieder Mugele. 2009. Hydrodynamic resistance of single confined moving drops in rectangular microchannels. *Lab Chip* 9, 7 (2009), 982–990.
- [38] Junchao Wang, Victor GJ Rodgers, Philip Brisk, and William H Grover. 2017. Instantaneous simulation of fluids and particles in complex microfluidic devices. *PLOS ONE* 12, 12 (2017), 1–14.
- [39] Wei Wang, Chun Yang, and Chang Ming Li. 2009. On-demand microfluidic droplet trapping and fusion for on-chip static droplet assays. *Lab Chip* 9, 11 (2009), 1504–1506.
- [40] Martin Wörner. 2012. Numerical modeling of multiphase flows in microfluidics and micro process engineering: a review of methods and applications. *Microfluid. Nanofluid.* 12, 6 (2012), 841–886.

APPENDIX

Symbols

ΔP	pressure gradient
Q	volumetric flow rate
R_c	resistance of a channel without droplets
l_c	channel length
w_c	channel width
h_c	channel height
μ_{cont}	fluid viscosity of the carrier fluid
R_d	resistance of a droplet
L_d	droplet length
R^*	resistance of a microchannel with droplets
v_d	speed of the droplet
α	slip factor
ΔP_{Lap}	Laplace pressure
γ	interfacial tension
r_d	droplet radius